increase the ICB effect. The reactions involving NiEDTA, Ni(trien), and NiBPEDA all have nickel-nitrogen bond rupture as rate determining while the ZnEDTA system involves copper-ligand bond formation as rate determining. Of the three possible explanations for the increased activity due to $CuOH^+$, the first, an increase in the stability of the dinuclear intermediate, cannot explain why $CuOH^+$ reacts at an accelerated rate with ZnEDTA because the dinuclear intermediate forms after the rate-determining step. The second explanation, a transition state, could explain all four systems but is based on the tenuous grounds of an acceleration in copper water loss due to hydroxide. The third possibility, however, fits all four cases since a hydrogen-bonded or hydroxide-bridged intermediate would affect the values of K_{os}, the outer-sphere association constant, to the same extent that it would affect the stability of a dinuclear intermediate. Therefore it is suggested that this is the most likely explanation for the increased reactivity of $CuOH^+$.

Registry No. $NiAEAMP^{2+}$, 52613-52-2; $NiBPEDA^{2+}$, 52613-53-3; Cu^{2+}, 15158-11-9; $CuOH^+$, 19650-79-4; $Cu_2(OH)_2^{2+}$, 12331-89-4.

Contribution from the School of Chemical Sciences, University of Illinois, Urbana, Illinois 61801

Magnetic Exchange Interactions in Transition Metal Dimers. III. Nickel(II) Di-μ-cyanato, Di-μ-thiocyanato, and Di-μ-selenocyanato Complexes and Related Outer-Sphere Copper(II) Complexes

D. MICHAEL DUGGAN[1] and DAVID N. HENDRICKSON*[2]

Received April 23, 1974 AIC40271X

Complexes with the general formulation $[M_2(tren)_2X_2](BPh_4)_2$, where M = Cu(II) and Ni(II), tren = 2,2′,2″-triaminotriethylamine, and $X^- = OCN^-$, SCN^-, and $SeCN^-$, have been prepared and studied by various physical techniques including magnetic susceptibility and esr. The nickel systems are dimeric with two X anions end-to-end bridging such that the nickel atoms are octahedrally coordinated. There is an antiferromagnetic exchange interaction ($J = -4.4$ cm^{-1}) in the cyanate-bridged nickel dimer, whereas both the di-μ-thiocyanate and the di-μ-selenocyanate systems are ferromagnetically coupled ($J = +2.4$ and $+1.6$ cm^{-1}, respectively). The exchange interaction in these nickel(II) dimers is discussed in terms of the known structural characteristics of the cyanate and thiocyanate dimers. The coordination geometry for the three XCN^-–Cu^{II} systems is shown to be trigonal bipyramidal by esr studies. Single-crystal X-ray work on one of the *two* forms of $[Cu_2(tren)_2(OCN)_2](BPh_4)_2$ substantiates this and shows that the copper cation in this compound is a dimer (Cu–Cu distance 6.58 Å) by virtue of the cyanate, which is N bonded to one trigonal-bipyramidal copper in the axial position, hydrogen bonding through its oxygen atom with one of the nitrogen atoms of the tren ligand coordinated to the second copper atom. The second form of copper cyanate probably has a somewhat different hydrogen-bonding configuration as a result of a different packing arrangement of copper dimers and tetraphenylborates. While there is no exchange interaction detectable for the $[Cu_2(tren)_2(XCN)_2](BPh_4)_2$ compounds in the magnetic susceptibility to 4.2°K, $\Delta M_S = 2$ transitions are seen in the esr spectra of the cyanate and thiocyanate complexes. Additional evidence for the dimeric nature of these copper complexes is found in the identification of esr transitions between their singlet and triplet states (in the $|SM_S\rangle$ coupled notation, $|1\ -1\rangle \rightarrow |00\rangle$ at high field and $|00\rangle \rightarrow |11\rangle$ at low field). The field position of these transitions for the copper thiocyanate dimer gives $|J| = 0.06$ cm^{-1}. The two different crystalline forms of $[Cu_2(tren)_2(OCN)_2](BPh_4)_2$ have $\Delta M_S = 2$ transitions and temperature-dependent singlet-to-triplet (S → T) transitions. Between 330 and 95°K the J value [from S → T transition] for one form varies between 0.09 and 0.16 cm^{-1}, while for the second form J varies between 0.05 and 0.06 cm^{-1}. Off-axis extrema are seen in the $\Delta M_S = 1$ region Q-band powder spectra for the three XCN–Cu outer-sphere dimers.

Introduction

In the previous two papers in this series[3,4] the symmetry, distance, and electron configurational effects influencing the magnitude and sign of magnetic exchange interactions in dimeric transition metal complexes have been illustrated. Exchange interactions that are propagated by discrete polyatomic bridging moieties between two paramagnetic centers have been the major concern. The present paper deals with magnetic interactions in both nickel(II) and copper(II) dimers where the metals are dibridged by either cyanate, thiocyanate, or selenocyanate groups. Interesting relationships between rather subtle changes in molecular structure and the net electron-exchange interaction have been detected. Particularly important is the series of di-μ-azido-, di-μ-cyanato-, di-μ-thiocyanato-, and di-μ-selenocyanato-bridged nickel(II) dimers (we have reported on the di-μ-azido material previously[4]). The bonding and resultant molecular structural differences in this Ni(II) series lead to both net antiferromagnetic (N_3^- and OCN^-) and ferromagnetic (SCN^- and $SeCN^-$) exchange interactions, the mechanisms for which will be discussed in this paper.

The chemistry and bonding properties of the pseudohalides OCN^-, SCN^-, and $SeCN^-$ have been the subject of several reviews[5,6] which focus upon the ability of these pseudohalides to coordinate to metals in a variety of ways. When the metal to anion ratio is 1:1, there are seven di-μ-XCN^- bridging possibilities; the three symmetric and most probable bridging modes are I–III.

(1) Esso Fellow, 1971–1972; Mobil Fellow, 1972–1973.
(2) Camille and Henry Dreyfus Fellow, 1972–1977.
(3) D. M. Duggan, E. K. Barefield, and D. N. Hendrickson, *Inorg. Chem.*, 12, 985 (1973).
(4) D. M. Duggan and D. N. Hendrickson, *Inorg. Chem.*, 12, 2422 (1973).
(5) J. L. Burmeister, *Coord. Chem. Rev.*, 3, 225 (1968).
(6) A. H. Norbury and A. I. P. Sinha, *Quart. Rev., Chem. Soc.*, 24, 69 (1970).

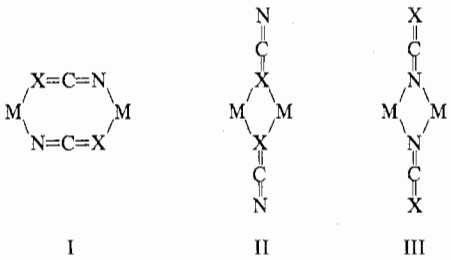

I II III

In our research we are investigating the occurrence of these different bonding possibilities for discrete transition metal dimers as well as characterizing the electronic structure of the various compounds. One of the compounds discussed in this paper, $[Ni_2(tren)_2(OCN)_2](BPh_4)_2$ where tren = 2,2′,2″-triaminotriethylamine, was recently shown to be a type I di-μ-cyanato-bridged dimer.[7,8] In fact, this is the *only* cyanate complex, to date, that has been proven by X-ray methods to contain a metal-oxygen bond. There are no known examples of di-μ-cyanato-bridged metal *dimers* with bridging mode II or III. Two mode I di-μ-thiocyanato dimer systems have been characterized by X-ray crystallographic techniques: $[Ni_2(en)_4(NCS)_2]I_2$,[9] where en is ethylenediamine, and the α and β isomers of $[Pt_2Cl_2(NCS)_2(P(n\text{-}C_3H_7)_3)_2]$.[10] Physical data have been used to implicate mode I di-μ-thiocyanate bridging in the anion[11] $[Co_2(NCS)_2(CN)_8]^{4-}$, the anion[12] $[Re_2(NCS)_8(PPh_3)_2]^{2-}$, and two Hg(II) systems.[13,14] There have been no crystal structure reports of di-μ-selenocyanate dimers.

The copper systems reported in this paper, $[Cu_2(tren)_2(XCN)_2](BPh_4)_2$, are most interesting in that while they show no observable exchange effects in the magnetic susceptibility experiment, their esr spectra exhibit $\Delta M_S = 2$ transitions as well as features associated with singlet-triplet transitions. Singlet-triplet transitions have been reported infrequently; examples are vanadyl tartrate dimer,[15] nearest-neighbor exchange-coupled Cu^{2+} ions doped into a potassium zinc sulfate lattice,[16] a Gd system,[17] and one discrete copper dimer.[18] The last case is seemingly not well substantiated. The importance of locating singlet-triplet transitions is due to their positions being a function of J, the exchange parameter. Finding such transitions for a series of related dimers allows the determination of the structural dependence of quite small values of J. Temperature and packing effects may be and in fact are observed.

Results and Discussion

Nickel Systems. In this paper we will be concerned with the compounds $[M_2(tren)_2(NCX)_2](BPh_4)_2$, where M = Cu(II), Ni(II) and X = O, S, Se. All work is reported on the tetraphenylborate salts not so much as a result of the desire to keep the anion the same but because it has been found that other anions frequently do *not* give the same dimeric compounds. As mentioned above, two X-ray crystal structures have been reported which are germane to this work: $[Ni_2(tren)_2(OCN)_2](BPh_4)_2$[7,8] and $[Ni_2(en)_4(SCN)_2]I_2$.[9] The latter is important because we will assume and substantiate with measurements that the structure of the cation is the same as that in $[Ni_2(tren)_2(SCN)_2](BPh_4)_2$. At the outset of this paper it is expeditious to review the molecular structure of these two di-NCX-bridged Ni(II) dimeric cations for we will refer to these structures frequently in the ensuing discussion.

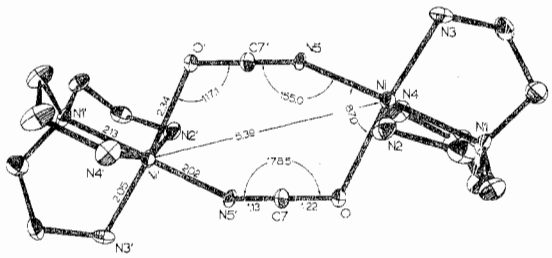

Figure 1. Molecular structure of the dimeric cation in $[Ni_2(tren)_2(OCN)_2](BPh_4)_2$ with coordination and bridge angles and distances. Hydrogen atoms are excluded.

Figure 1 shows the structure of the $[Ni_2(tren)_2(OCN)_2](BPh_4)_2$ dimer unit with pertinent angles and distances included. In $[Ni_2(tren)_2(OCN)_2](BPh_4)_2$ the bridge consists of two parallel cyanate groups with the nickel atoms situated above and below the plane of the cyanates by approximately 0.25 Å. The Ni-Ni distance is 5.39 Å; the NiOC and CNNi angles are 117.1° and 155.0°, respectively, angles which fall between what would be expected for the two possible hybridization schemes for the OCN system.

The structure of the di-μ-thiocyanate cation is quite similar to that of the di-μ-cyanate, where the bridging unit is analogous, with sulfur substituted for oxygen. The metal-metal distance is 5.78 Å, reflecting the greater size of the sulfur atom, while the NiSC and CNNi angles are 100 and 167°, respectively (errors of several degrees may be attached to these figures reflecting the low accuracy of the structure). A CN bond distance of 1.18 Å is found which is somewhat larger than expected for a fully triply bonded pair. These factors taken together implicate a mode of bonding which cannot be described simply by any valence-bond formalism, although the best description might be that of Ginsberg, *et al.*,[19] based on the MO structure of the isoelectronic CO_2. In their analysis the small MSC angle is ascribed to the $e_g(Ni)$-$p_z(S)$ bonding being more important than that involving a nominally sp^3 or sp^2 hybridized sulfur. The nickel atoms in the di-μ-thiocyanate dimer are only 0.05 Å out of the plane of the thiocyanates.

In this section we discuss the structures and spectral and magnetic properties of the dimers $[Ni_2(tren)_2(OCN)_2](BPh_4)_2$, $[Ni_2(tren)_2(SCN)_2](BPh_4)_2$, and $[Ni_2(tren)_2(SeCN)_2](BPh_4)_2$. Analytical data are given in Table I.[20] While the magnetic exchange properties of di-μ-thiocyanato-bridged $[Ni_2(en)_4(SCN)_2]I_2$ have been investigated,[19] the spectral and magnetic properties of the analogous member of our series are reported for comparison purposes. The structure of

(7) D. M. Duggan and D. N. Hendrickson, *J. Chem. Soc., Chem. Commun.*, 411 (1973).
(8) D. M. Duggan and D. N. Hendrickson, *Inorg. Chem.*, 13, 2056 (1974).
(9) A. E. Shvelashvili, M. A. Porai-Koshits, and A. S. Antsyshkina, *J. Struct. Chem. USSR*, 10, 552 (1969).
(10) U. A. Gregory, J. A. J. Jarvis, B. T. Kilbourn, and P. G. Owston, *J. Chem. Soc. A*, 2770 (1970); J. Chatt and F. A. Hart, *J. Chem. Soc.*, 1416 (1961); J. Chatt, L. A. Duncanson, F. A. Hart, and P. G. Owston, *Nature (London)*, 181, 43 (1958).
(11) J. L. Burmeister and Al-Janahi, *Inorg. Chem.*, 4, 962 (1965).
(12) F. A. Cotton, W. R. Robinson, R. A. Walton, and R. Whyman, *Inorg. Chem.*, 6, 929 (1967).
(13) A. R. Davis, C. J. Murphy, and R. A. Plane, *Inorg. Chem.*, 9, 423 (1970).
(14) I. S. Ahuja and A. Garg, *J. Inorg. Nucl. Chem.*, 34, 2074 (1972).
(15) P. G. James and G. R. Luckhurst, *Mol. Phys.*, 18, 141 (1970).
(16) D. J. Meredith and J. C. Gill, *Phys. Lett. A*, 25, 429 (1967).
(17) R. J. Birgeneau, M. T. Hutchings, and W. P. Wolf, *Phys. Rev. Lett.*, 17, 308 (1966).
(18) D. Y. Jeter and W. E. Hatfield, *Inorg. Chim. Acta*, 6, 440 (1972).
(19) A. P. Ginsberg, R. L. Martin, R. W. Brookes, and R. C. Sherwood, *Inorg. Chem.*, 11, 2884 (1972).
(20) See paragraph at end of paper regarding supplementary material.

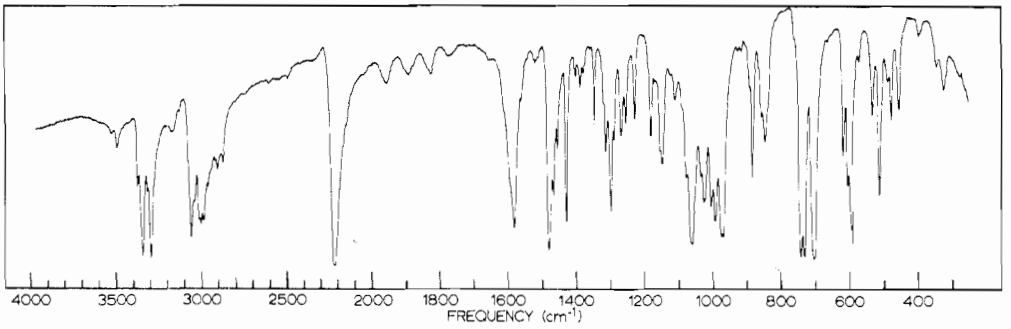

Figure 2. Infrared spectrum of $[Ni_2(tren)_2(OCN)_2](BPh_4)_2$ in a 13-mm KBr pellet.

the selenocyanate complex will be inferred from its spectral characteristics. It will be shown that the three nickel compounds are quite similar with respect to their ir and electronic spectra and thus in gross overall structure. There are small structural differences in the bridges, however, that give rise to distinctly varied magnetic properties.

There is, naturally, an abundance of ir data recorded in the literature for cyanate, thiocyanate, and selenocyanate compounds.[21] Each of these has three characteristic ir bands which are often observable and in many cases point to the bonding mode of the ion. There is a ν_{CN} absorption (or perhaps more accurately ν_a for the OCN case) close to 2000 cm^{-1}, a ν_{CX} absorption (ν_s for OCN) whose frequency depends upon X, and a lower frequency δ_{XCN} band which is doubly degenerate. The ν_{NH}, ν_{CN}, and, when seen, ν_{CX} bands for all nickel and copper compounds are summarized in Table II.[20] The full ir spectrum from 250 to 4000 cm^{-1} for $[Ni_2(tren)_2(OCN)_2](BPh_4)_2$ is given in Figure 2, and the spectral region from 1100 to 1400 cm^{-1} for all six OCN^-, SCN^-, and $SeCN^-$ nickel and copper compounds is shown in Figure 3.

Considerable discussion has appeared concerning the probable location of vibrational bands for an end-to-end (mode I) bonded cyanate, yet no data have been reported for a molecule which has been proven by X-ray crystallography to have this structure. The compound $[Ni_2(tren)_2(NCO)_2](BPh_4)_2$ fills this requirement. From Table II and Figure 2 it is seen that for this complex $\nu_a = 2217$ cm^{-1}. A comparison of the 1100–1400 cm^{-1} regions of the three NCX nickel systems (see Figure 3) shows that $\nu_s = 1297$ cm^{-1} for the di-μ-cyanate compound. The ν_a (2217 cm^{-1}) value proves to be well within the range (see ref 21) observed for nitrogen-bonded cyanates. Thus, the suggestion[22] that this frequency should increase upon M–NCO–M bridging, while possibly true, is *not* a useful criterion. Of greatest interest is the ν_s vibration, which has long been used[21,23,24] to indicate oxygen bonding in the case of a decreased ν_s frequency. While 1297 cm^{-1} *is* slightly lower than the range of N-bonded complexes (1300–1350 cm^{-1}), those complexes thought to have oxygen bonding or mode I bridging[23] have much lower (~1200 cm^{-1}) frequencies. Again we must point out the important conclusion that while low ν_s frequencies *may* be characteristic of some oxygen-bound or end-to-end bridged cyanates, such a decreased frequency is not a *necessary* condition for proposing such a structure. It should be mentioned that due to the possibility of the bending overtone $2\delta_{NCO}$ mixing with the ν_s vibration, Fermi resonance may split the ν_s into two bands, as proposed by Bailey and Kozak[23] for $[Ph_4As]_3[Mo(OCN)_6]$, where they found bands at 1296 and 1140 cm^{-1}. There is, however, no band in our spectrum of $[Ni_2(tren)_2(OCN)_2](BPh_4)_2$ that we can identify as the lower component of such a doublet. Therefore, we must conclude that 1297 cm^{-1} is the actual position of the absorption, and no Fermi resonance occurs.

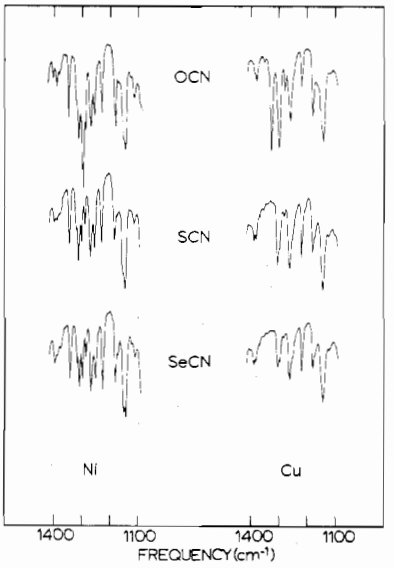

Figure 3. Infrared spectra from 1100 to 1400 cm^{-1} for $[M_2(tren)_2X_2](BPh_4)_2$ (M = Cu, Ni; X = OCN, SCN, SeCN). All samples prepared as KBr pellets.

With the exception of those bands due to the SCN^- and $SeCN^-$ groups, the ir spectra of $[Ni_2(tren)_2(SCN)_2](BPh_4)_2$ and $[Ni_2(tren)_2(SeCN)_2](BPh_4)_2$ are almost indistinguishable from that of the cyanate complex. The low-intensity features in the ν_{NH} region of the cyanate (see Table II) are the only exceptions, and these weak bands seem merely to indicate a small distortion, such as was evident in the μ-oxalato $[M_2(tren)_2(C_2O_4)](BPh_4)_2$ spectra described in ref 3. In both the SCN^- and $SeCN^-$ systems only the ν_{CN} bridge vibration can be located and in each case the ν_{CN} values fall in regions previously taken to be indicative of end-to-end bridge systems.[23] Infrared evidence points to the fact that all three of the nickel systems are isostructural and by comparison with the known structure[7,8] of $[Ni_2(tren)_2(OCN)_2](BPh_4)_2$ are all type I bridged. As indicated in the previous two sections, this is not the first instance of a type I di-μ-thiocyanate system, whereas for $SeCN^-$ this is the first reported doubly bridged metal dimer.

Electronic absorption spectra were run for solid samples (KBr pellets) of the three nickel dimers; the data are given in

(21) R. A. Bailey, S. L. Kozak, T. W. Michelson, and W. N. Mills, *Coord. Chem. Rev.*, 6, 407 (1971).

(22) A. Yu. Tsivadze, G. V. Tsintsadze, Yu. Ya. Kharitonov, A. M. Golub, and A. M. Mamulashvili, *Zh. Neorg. Khim.*, 15, 1818 (1970).

(23) R. A. Bailey and S. L. Kozak, *J. Inorg. Nucl. Chem.*, 11, 689 (1969).

(24) G. V. Tsintsadze, A. Yu. Tsivadze, and Ts. L. Makhatadze, *Soobshch. Akad. Nauk Gruz. SSR*, 56, 301 (1969).

Table III. Electronic Spectral Data for $[M_2(tren)_2(XCN)_2](BPh_4)_2$ (M = Ni, Cu; X = O, S, Se)

M	X	λ, Å	$\bar{\nu}$, kk	Intens
Ni	O	3700	27.0	m
		5700	17.54	m
		7900	12.66	w, sp
		(9000)	11.1	s, vbr
Ni	S	(3800)	26.3	sh
		5700	17.54	m
		7900	12.66	w, sp
		(8700)	11.5	s, vbr
Ni	Se	5700	17.54	m
		8100	12.35	w, sp
		8700	11.5	s, vbr
Cu	O	6700	14.9	mw, sh
		8800[a]	11.4	s, vbr
Cu	S	6650	15.0	mw, sh
		8450[a]	11.8	s, vbr
Cu	Se	6550	15.3	mw, sh
		8600[a]	11.6	s, vbr

[a] This band is asymmetric, indicating a shouldering band at ~10,000 Å.

Table III. Only solid-state spectra are reported, because molecular weight studies indicated dissociation in solution. In each case, the three lowest energy bands (~11.5, 12.5, and 17.5 kK) correspond to the $^3A_{2g}(F) \rightarrow {}^3T_{2g}(F)$, $^1E_g(P)$, and $^3T_{1g}(F)$ transitions, respectively, of a d^8 ion in an octahedral field. The higher energy $^3A_{2g}(F) \rightarrow {}^3T_{1g}(P)$ band is sometimes difficult to see in the solid state (dispersion, ligand absorptions, etc.) and is only reported for two of the nickel dimers. The ~11.5-kK band in all three systems is extremely broad and cannot be located accurately, whereas the positions of the next two higher energy bands are more easily determined due to their sharpness (the $^1E_{1g}$ is, of course, spin forbidden and therefore weak, but sharp). Least-squares fitting of the ^1E_g and ^3T bands to the d^8 electrostatic matrix elements given in ref 25 indicates that while *Dq* is essentially constant (~1160 cm^{-1}) for the three systems, the interelectron repulsion parameter *B* is fairly similar for the SCN^- and $SeCN^-$ systems but larger for the cyanate (734, 735, and 817 cm^{-1}, respectively). The decrease in *B* could be taken as evidence that there is a decrease in covalency between the metal and the X atom of the XCN bridging moiety in the series OCN < SCN ~ SeCN.

To further characterize the structure of the three nickel dimers, X-ray powder pattern data were recorded for them, and two interesting observations made. First, two different crystalline forms of $[Ni_2(tren)_2(OCN)_2](BPh_4)_2$ have been identified. The powdered $[Ni_2(tren)_2(OCN)_2](BPh_4)_2$ that precipitates from an aqueous solution of Ni^{2+}, tren, and NCO^- upon addition of BPh_4^- gives an X-ray powder pattern different from that of the crystalline $[Ni_2(tren)_2(OCN)_2](BPh_4)_2$ which is obtained by evaporation of an acetonitrile solution of the powdered compound. Magnetic susceptibility and ir measurements on both materials indicate that the *same* dimeric cation is present in each, while it is just the packing of these ions into the crystal lattice that is different. This points out that while the unexpected existence of the Ni–OCN–Ni bridging in this system can be explained in terms of favorable packing with the BPh_4^- counterion, it is unlikely that there should be *two* such favorable packing arrangements unless the dimer itself is a fairly stable entity. It has been shown,[8] however, that the BPh_4^- anion is in a relatively stable configuration in the crystallized form, demonstrating favorable packing is this case. It has been secondly noticed from the nickel powder patterns that the SCN^- and $SeCN^-$ complexes crystallize in quite similar unit cells. The positions of all the powder pattern lines for these two complexes are within 0.2° (2θ, Cu Kα radiation) of each other; however, the intensities are only approximately corresponding, a difference undoubtedly attributable to the greater scattering power of the Se atom as well as to slight shifting in the packing arrangement. The two nickel cyanate *crystal* forms both are apparently different from those of the SCN^- and $SeCN^-$ complexes. In summary, the nickel di-μ-cyanate and di-μ-thiocyanate dimers have been directly or indirectly characterized by single-crystal X-ray work to have end-to-end type I bridging. From the above discussion it is apparent that the di-μ-selenocyanate nickel dimer also has a similar structure.

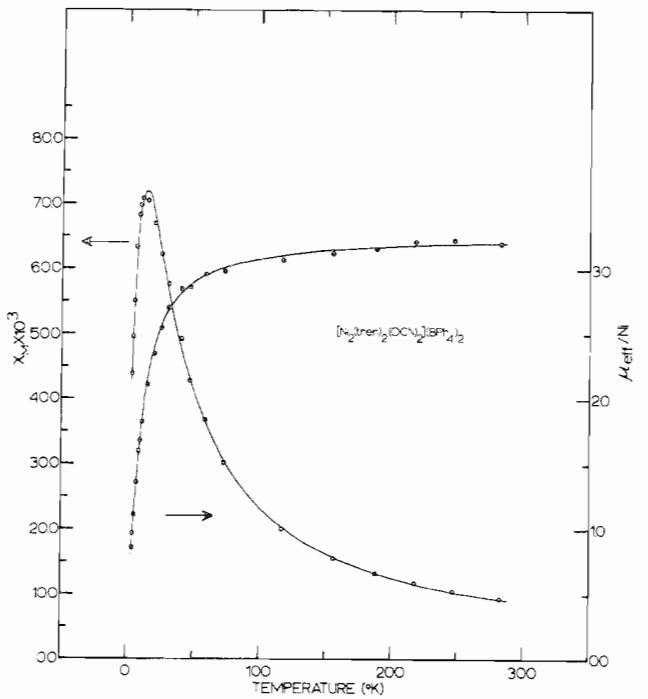

Figure 4. Experimental and calculated magnetic susceptibility data for $[Ni_2(tren)_2(OCN)_2](BPh_4)_2$. The lines are calculated from the parameters shown in Table V.

The results of variable-temperature (4.2–283°K) magnetic measurements for the three nickel dimers are given in Table IV[20] and Figures 4 and 5. The effective magnetic moment (μ_{eff}) *vs.* temperature curves are plotted for all three systems, whereas the molar paramagnetic susceptibility (χ_M) *vs.* temperature curve is only given for the cyanate compound. In short, while the magnetic curves of two of the compounds (SCN^- and $SeCN^-$) show indications of *intra*dimer ferromagnetic coupling (Figure 5), the curve for the cyanate has a distinct antiferromagnetic transition (Figure 4). The cyanate susceptibility increases with decreasing temperature until a maximum is reached at 14°K, whereupon it decreases rapidly to 4.2°K. This rapid decrease in χ_M from 14 to 4.2°K is indicative[4] of a sample which is relatively free of paramagnetic impurities. The magnetic susceptibility data for $[Ni_2(tren)_2(OCN)_2](BPh_4)_2$ were least-squares fit to Ginsberg's[19] equation for a nickel dimer; calculational details are given in ref 3. The theoretical equations account for an *intra*dimer exchange integral *J* and nickel(II) single-ion zero-field splitting *D*, as well as an *inter*molecular magnetic exchange as per the molecular field approximation. This last interaction is gauged by *Z'J'*, where *Z'* is the lattice "coordination number" of each dimer and *J'* is the *inter*molecular exchange

(25) J. S. Griffith, "The Theory of Transition Metal Ions," Cambridge University Press, London, 1964, p 410.

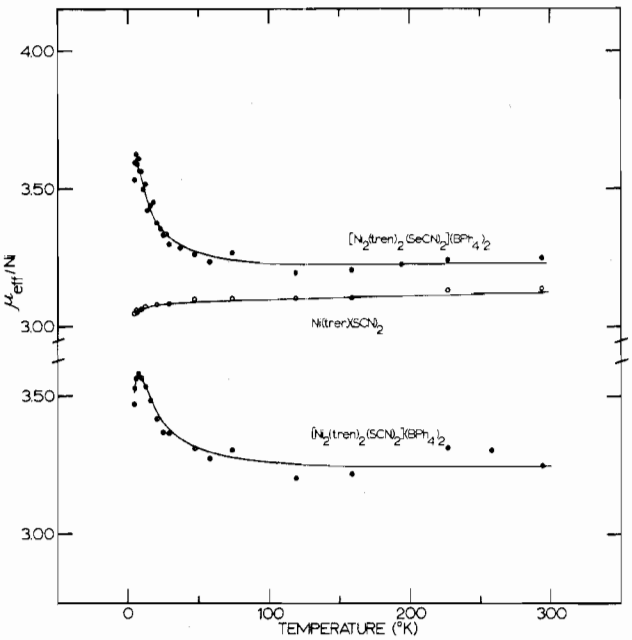

Figure 5. Experimental and calculated magnetic susceptibility data for $[Ni_2(tren)_2(SeCN)_2](BPh_4)_2$ (top), Ni(tren)$(SCN)_2$ (middle), and $[Ni_2(tren)_2(SCN)_2](BPh_4)_2$ (bottom). The lines are calculated from the parameters shown in Table V.

Table V. Magnetic Susceptibility Fitting Parameters for $[Ni_2(tren)_2(XCN)_2](BPh_4)_2$ (X = O, S, Se) and Ni(tren)$(SCN)_2$[a]

	J, cm^{-1}	g	D, cm^{-1}	$Z'J'$, cm^{-1}	SE[b]
$[Ni_2(tren)_2(OCN)_2](BPh_4)_2$	−4.4	2.282	−10.1	0.71	0.025
$[Ni_2(tren)_2(SCN)_2](BPh_4)_2$	+2.4	2.255	−0.45	−0.16	0.034
$[Ni_2(tren)_2(SeCN)_2](BPh_4)_2$	+1.6	2.247	−0.49	−0.07	0.035
Ni(tren)$(SCN)_2$	0.0	2.181	−0.76	−0.02	0.009

[a] See text for equations and references. [b] SE = $\{\Sigma_{i=1}^{n}[\mu_{eff}(obsd)_i - \mu_{eff}(calcd)_i]^2/(n-K)\}^{1/2}$, where n is the number of observables and K is the numbers of parameters.

integral. In addition, the nickel ion is assumed to be magnetically isotropic (*i.e.*, $g_x = g_y = g_z \equiv g$) and the temperature-independent paramagnetism was taken as 200×10^{-6} cgsu/mol of dimer. The solid lines in Figure 4 illustrate the success of the theoretical fitting, where in the cyanate case the best fit was obtained with $J = -4.41$ cm^{-1}, $g = 2.28$, $D = -10.1$ cm^{-1}, and $Z'J' = +0.71$ cm^{-1} (the D value was incorrectly reported previously[7]). The D value is probably overestimated; it is not expected to be accurately determined,[3,19] nor will its magnitude have a significant effect on the size of J, which is probably correct within 0.3 cm^{-1}.

It is clear from Figures 4 and 5 and Table IV[20] that the $[Ni_2(tren)_2(SCN)_2](BPh_4)_2$ and $[Ni_2(tren)_2(SeCN)_2](BPh_4)_2$ systems are quite different from the cyanate complex in their magnetic behavior. Their magnetic moments do not fall with decreasing temperature but, on the contrary, rise slightly. This is, as reported by Ginsberg, *et al.*,[19] for the analogous $[Ni_2(en)_4(SCN)_2]I_2$, indicative of ferromagnetic exchange coupling between the two nickel atoms in these dimers. Fitting of the SCN$^-$ and SeCN$^-$ data gives for $[Ni_2(tren)_2(SCN)_2](BPh_4)_2$ $J = +2.4$ cm^{-1}, $g = 2.255$, $D = -0.45$ cm^{-1}, and $Z'J' = 0.16$ cm^{-1} and for $[Ni_2(tren)_2(SeCN)_2](BPh_4)_2$ $J = +1.6$ cm^{-1}, $g = 2.247$, $D = -0.49$ cm^{-1}, and $Z'J' = 0.07$ cm^{-1}. In the case of $[Ni_2(en)_4(SCN)_2]I_2$, analysis of the magnetism data to 1.6°K gives[19] $J = 4.5$ cm^{-1}, $g = 2.14$, $D = -3.3$ cm^{-1}, and $Z'J' = -0.15$ cm^{-1}. The fitting parameters for all three Ni–tren compounds are given in Table V. Unfortunately, we do not presently have the facilities to go to lower temperatures than 4.2°K to allow a better fitting of the parameters in this region.

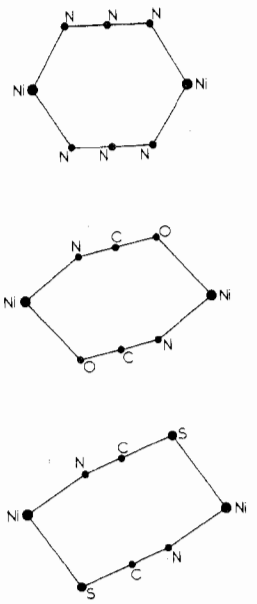

Figure 6. Diagramatic representation of the bridging structures of di-μ-azide, -cyanate, and -thiocyanate systems. The cyanate and thiocyanate dimensions are taken from crystallographic studies referenced in the text while the structure of the azide system is suggested by spectroscopic studies (see ref 4).

The shapes of the susceptibility curves for the $[Ni_2(tren)_2(SCN)_2](BPh_4)_2$ and $[Ni_2(tren)_2)SeCN)_2](BPh_4)_2$ do not lend themselves to accurate fitting of the D and $Z'J'$ parameters and as such for these ferromagnetic systems the J values are probably determined to no better than 1 cm^{-1}. That there *is* a clearly defined ferromagnetic exchange for the SCN and SeCN$^-$ dimers is proven by comparison of the μ_{eff} curves to that for monomeric Ni(tren)$(SCN)_2$ (see Figure 5). Our limitations in accuracy in J preclude only accurate relative assessments of exchange for the SCN$^-$ and SeCN$^-$ cases and as such we consider them to be essentially the same.

From the spectroscopy and magnetism of these three nickel systems it may be concluded that while all three are basically similar in gross structural features, it is the precise geometry of the bridging system that determines the magnetic exchange properties. In the remainder of this section we will discuss the factors determining the sign and magnitude of J for the $[Ni_2(tren)_2(XCN)_2](BPh_4)_2$ (X = O, S, Se) compounds as well as for $[Ni_2(tren)_2(N_3)_2](BPh_4)_2$. Figure 6 shows a plane projection of three of the nickel-bridging units. The details of the structures of the cyanate and thiocyanate systems have been given in the above discussion. The selenocyanate system, the structure for which is not indicated in Figure 6, probably has a structure similar to the thiocyanate case as per the above discussion.

An analysis of the variability of exchange in the above four nickel(II) dimers can be formulated in terms of two general factors. First, it is important to know the orientation, with respect to the bridging structure, of the metal "d orbitals" containing the unpaired electron (*i.e.*, orientation between g tensor and Ni–Ni vector). Because we are dealing with the same backside ligand (*i.e.*, tren) in all four Ni(II) complexes, it is reasonable to assume that no variability in **g** tensor orientation attributable to backside ligand is introduced in the series. The degree of planarity of the four bridging units, however, is somewhat variable. For example, the two nickel atoms are above and below, respectively, the plane of

the two cyanates by 0.25 Å, whereas the two nickel atoms in the thiocyanate unit are above and below the plane of the thiocyanates by only 0.05 Å. Considering the size of the selenium atoms, it is probably fair to extrapolate to an essentially planar bridging unit in the case of $NCSe^-$. [Preliminary X-ray results from Professor C. Pierpont indicate that the nickel atoms in the $[Ni_2(tren)_2(N_3)_2]^{2+}$ ion are approximately 0.5 Å above and below the plane formed by all six bridging nitrogens.] We will assume that the deviations from planarity in all four nickel(II) dimers are not important and as such the variability in orientation, with respect to the bridge structure, of the metal **g** tensor is not the most important factor causing the change in J values in the series.

The second and, in our opinion, most important factor in determining J in this series is the symmetry and energies of the bridge molecular orbitals. It is just these orbitals that, in conjunction with the metal center orbitals, determine the bridging unit structural changes pictorially represented in Figure 6. In the second paper in this series[4] it was suggested that for a *symmetric* bridging situation (*i.e.*, where there is a mirror plane perpendicular to the metal-metal vector) there are no first-order ferromagnetic exchange pathways. This is because the metal ions are restricted by symmetry to bond into the same bridge molecular orbitals leading to a pairing of electrons, that is, an antiferromagnetic coupling.

For the azide-bridged nickel dimer $[Ni_2(tren)_2(N_3)_2](BPh_4)_2$[4] the exchange integral J is -35 cm^{-1}, indicative of a moderate *antiferromagnetic* exchange. This observation fits the above proposal in that the bridge geometry is symmetric (strictly, only has mirror plane perpendicular to Ni-Ni vector if planar). Changing the bridge from azide to cyanate (center, Figure 6) leads to a bridging unit which is no longer symmetric, and now the two nickel atoms bond into bridge orbitals that are *not* of necessity of equal construction with respect to the two metal centers. As a result there are both antiferromagnetic and ferromagnetic pathways possible in the di-μ-cyanate system. The *net* exchange interaction in this dimer is found to be weakly antiferromagnetic to the extent of $J = -4.4$ cm^{-1}. That is, the attenuation in antiferromagnetic exchange in going from the N_3^- to the OCN^- system is due to spin-polarization "pathways" where one nickel atom is interacting with a given bridge orbital which is orthogonal to a bridge interacting with the unpaired electron density on the second nickel atom. Ferromagnetic "pathways" are thus associated with any spin-polarization pathway which has an orthogonal interaction.

In the case of the thiocyanate-bridged dimer the transition from strong symmetry to strong antisymmetry has reached the point where the nickel-bridge bonding is so different for the two ends of each bridging anion that a *net* ferromagnetic exchange is observed. Ginsberg, *et al.*,[19] described the bonding in $[Ni_2(en)_4(SCN)_2]I_2$ as $Ni(e_g)$-$\sigma^b(N)$ at one bridge end and $Ni(e_g')$-$\pi^b(S)$ at the other, the orthogonality between the σ and π bridge orbitals dictating the quintet ground state. The selenocyanate-bridged dimer has essentially the same sign and magnitude of exchange as the thiocyanate and thus probably the same bridging geometry. It may be concluded that, in the case of linear bridged dimers, it is the difference in Ni-bridge bonding at the two bridge ends that primarily determines the nature of the exchange interaction. When the two terminal bridge atoms are of different size, the bonding at the large atom will be more angular and will enforce a net ferromagnetic interaction.

Copper Systems. We have obtained the single-crystal X-ray structure of one of the *two* forms of $[Cu_2(tren)_2(NCO)_2](BPh_4)_2$ and in this section various physical data will be presented to show that $[Cu_2(tren)_2(SCN)_2](BPh_4)_2$, $[Cu_2(tren)_2(SeCN)_2](BPh_4)_2$, and even $[Cu_2(tren)_2(N_3)_2](BPh_4)_2$[4] have very similar structures. This will be followed by some very interesting esr data bearing on the dimeric nature of the copper dications in these tetraphenylborate salts.

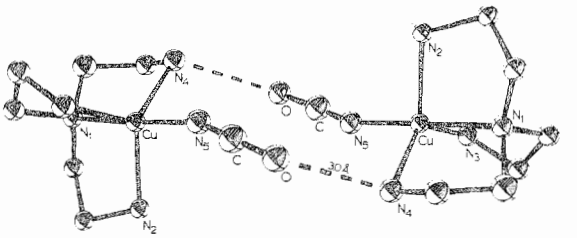

Figure 7. Molecular structure of the dimer cation in form I of $[Cu_2(tren)_2(OCN)_2](BPh_4)_2$ after refinement of atomic positions with isotropic thermal parameters. The hydrogen-bonding contact is indicated by a dashed line.

The compound $[Cu_2(tren)_2(OCN)_2](BPh_4)_2$ crystallizes in the $P2_1/c$ space group with $a = 14.003$ (6) Å, $b = 10.399$ (5) Å, $c = 20.436$ (9) Å, and $\beta = 94.01$ (3)°. Some 1912 reflections (1212 observed) were collected with a computer-automated diffractometer, refinement with an isotropic model without hydrogen atoms having progressed to a weighted $R = 0.089$. The structural features of the dimer $[Cu_2(tren)_2(OCN)_2]^{2+}$ are shown in Figure 7; the dimer sits on a center of inversion in the unit cell. The molecular structural characteristics of the cyanate dimer are very similar to those we recently found[26] for the copper dimer in $[Cu_2(tren)_2(CN)_2](BPh_4)_2$. As can be seen in Figure 7, the halves of the cyanate dimer are bridged solely by means of two N-H···O hydrogen-bonding contacts between a cyanate oxygen and a tren ligand. The 2.95-Å N-O distance is very reasonable for such a hydrogen bond. Although the bridging hydrogen cannot be seen, its position can be calculated (assuming sp^3-hybridized nitrogen) from the M-N-C(tren) angle to be ~0.2 Å from the N-O vector.

The study of this copper system is a study of magnetic exchange propagated through a hydrogen bond or, alternatively, a study of electron exchange between the two metal centers of an *outer-sphere* association of two trigonal-bipyramidal copper(II) complexes. Spectral evidence as to the similarity of molecular structure of the two other XCN (X = S, Se) copper(II) systems with this form of $[Cu_2(tren)_2(OCN)_2](BPh_4)_2$ (we will call this form I) will be presented before the results of the electron-exchange study are delineated. Physical data bearing on and speculation as to the structure of form II of copper(II) cyanate will appear later. The immediately following spectroscopic discussion applies to both forms I and II of the cyanate, unless stated otherwise.

Infrared data for the N-H and XCN vibrations of the three Cu^{II}-NCX (X = O, S, Se) systems are presented in Table II,[20] and the 1100-1400-cm^{-1} regions of all three copper complexes are illustrated in Figure 3. It has been our experience that the 1100-1400-cm^{-1} region is indicative of the tren coordination stereochemistry about the metal. As noted above, all three of the nickel systems have similar 1100-1400-cm^{-1} patterns with the cyanate having an additional ν_s(OCN) feature. The copper systems exhibit a pattern that is distinctly different from the nickel pattern and further is very similar for all three cases with the copper cyanate having the additional ν_s(OCN) feature. The copper pat-

(26) D. M. Duggan, R. G. Jungst, K. R. Mann, G. D. Stucky, and D. N. Hendrickson, *J. Amer. Chem. Soc.*, 96, 3443 (1974); D. M. Duggan and D. N. Hendrickson, *Inorg. Chem.*, 13, 1911 (1974).

tern is simpler than the nickel because in the copper systems the symmetry of the tren moiety is higher, approximating C_{3v}. The similarity of pattern in the copper spectra, taken together with the known structure of $[Cu_2(tren)_2(OCN)_2](BPh_4)_2$ implies that the SCN^- and $SeCN^-$ analogs have very similar stereochemistries; that is, they also have trigonal-bipyramidal copper centers. In agreement with this we have found that similar 1100–1400 cm^{-1} patterns are to be found for $[Cu_2(tren)_2(CN)_2](BPh_4)_2$[26] and $[Cu(tren)(SCN)](SCN)$,[27] both of which are known to have trigonal-bipyramidal copper. It is probably not possible to draw a conclusion from the 1100–1400-cm^{-1} patterns as to whether the Cu-NCS or Cu-NCSe systems are dimeric (*via* hydrogen bonding) or not. The $\nu_a(NCO)$ vibration in the copper cyanate complex can be seen at 2217 cm^{-1}, which is the same as reported[8] for $[Ni_2(tren)_2(OCN)_2](BPh_4)_2$ where *both* ends of the cyanate are coordinated to the metal. It is interesting to note that the copper cyanate $\nu_s(OCN)$ band which is seen at 1329 cm^{-1} is some 32 cm^{-1} higher energy than the nickel $\nu_s(NCO)$.

The copper thiocyanate complex has a ν_{CN} band at 2100 cm^{-1} and from a comparison of spectra in the copper series the ν_{CS} (804 cm^{-1}) and δ_{NCS} (520 cm^{-1}) bands have been located, the δ_{NCS} band position being somewhat uncertain due to overlapping of two weaker absorptions. The bridging or terminal character of the SCN group *cannot* be ascertained from these band positions. While the ν_{CS} and δ_{NCS} frequencies are consistent with M-NCS bonding, there are cases reported where bridging SCN^- groups have absorptions in these same regions. The ir spectrum of $[Cu_2(tren)_2(SeCN)_2](BPh_4)_2$ lends itself to an identification of ν_{CN} (2098 cm^{-1}) and ν_{CSe} (520 cm^{-1}) but not δ_{NCSe}; again it is not possible to tell whether the $SeCN^-$ group is involved in a hydrogen-bond bridge as is found for the NCO^- group. The difficulty in this determination is of course a reflection of the inherent weakness of hydrogen bonds relative to the X-C and C-N bonds in our system. Determination of the presence of hydrogen bonding by a study of the N-H vibrations has been unsuccessful.

Some support for proposing a hydrogen-bonded bridge (as found in the copper cyanate) for the SCN^- copper system can be gleaned from a comparison of single-crystal X-ray precession data for the two systems. The compound $[Cu_2(tren)_2(SCN)_2](BPh_4)_2$ appears to be isomorphous with $[Cu_2(tren)_2(OCN)_2](BPh_4)_2$; the former crystallizes in the $P2_1/c$ space group with $a = 14.91$ Å, $b = 9.68$ Å, $c = 20.77$ Å, and $\beta = 98.4°$. The cell dimensions of the Cu-NCS and Cu-NCO systems are very similar, with almost identical unit cell volumes. Moreover, the cell dimensions of hydrogen-bond bridged $[Cu_2(tren)_2(CN)_2](BPh_4)_2$[26] ($P2_1/c$, $a = 13.792$ (7) Å, $b = 10.338$ (6) Å, $c = 20.316$ (14) Å, $\beta = 94.27°$) are also similar; however, the unit cell volume of this cyanide complex is, as expected, smaller than those for the Cu-NCS and Cu-NCO systems. It is thus reasonable to assume on this basis that the cation in the Cu-NCS compound possesses a hydrogen-bonded dimeric structure. Finally, comparison of X-ray powder patterns of $[Cu_2(tren)_2(SCN)_2](BPh_4)_2$ and $[Cu_2(tren)_2(SeCN)_2](BPh_4)_2$ shows that the four most intense features, although they are of differing intensity, are coincidental from one pattern to another.

The broadness and overlapping characteristics of the electronic absorptions of the NCX copper compounds make it difficult to locate and assign individual bands (see comments in the Experimental Section on the influence of experimental technique on the quality and appearance of spectra obtained from KBr pellets). For each of the three copper complexes there are three bands (see Table III), one intense broad band at ~8600 Å and one higher and one lower energy shoulder. The lower energy shoulder is so broad and close to the central peak that it is frequently apparent only due to the asymmetry it imposes on the intense band. On the contrary, the higher energy shoulder is better resolved. Trigonal-bipyramidal copper(II) generally has the following ordering of states: $^2A'(d_{z^2}) < {}^2E'(d_{x^2-y^2}, d_{xy}) < {}^2E''(d_{xz}, d_{yz})$.[28] Under the effects of spin-orbit coupling both of the E states split and the energy level scheme of Chart I is obtained (the Γ designations are irreducible representations of the D_3' double group). In this scheme λ is the spin-orbit coupling constant. There are only three dipole-allowed electronic transitions from the Γ_7 ground state, $\Gamma_7(A') \rightarrow \Gamma_8(E')$, $\Gamma_9(E')$ and $\Gamma_9(E'')$, and these are likely to be the origins of our three observed absorptions. Since the splittings between the two lowest energy bands are small (~1-2 kK), it seems that this splitting is largely due to spin-orbit interaction in the $^2E'$ state ($\lambda \simeq -830$ cm^{-1}) and that there is little additional splitting due to distortion from trigonal symmetry. Assignment of these spectra to a trigonal-bipyramidal scheme only implies that the data are consistent with that structure. Due to overlapping of the bands and the lack of polarization data, no structure can be uniquely determined; however, the similarity of the Cu-NCS and Cu-NCSe data to those for Cu-NCO implies a similarity of structure.

Q-Band esr spectra (summarized in Table VI) provide evidence as to the dimeric (*i.e.*, relatively short Cu-Cu distance) nature of the $[Cu_2(tren)_2(NCX)_2](BPh_4)_2$ (X = O, S, Se) compounds. The Q-band esr data for the cyanate complex are presented first because the structure of form I of the copper cyanate compound is known. The presence of two

Chart I

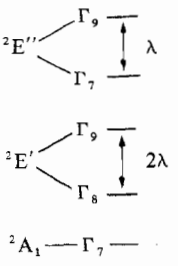

Table VI. Summary of Esr Data for $[Cu_2(tren)_2(XCN)_2](BPh_4)_2$ (X = O, S, Se)[a]

Compd	"Best" guesses[b]		Other features[c]		
	$g_\perp$	$g_\parallel$	g_4	g_5	g_6
X = O, form I					
Room temp	2.146	2.008	2.215	2.082	
Liquid N_2	2.146	2.017	2.245	2.097	2.070
X = O, form II					
Room temp	2.153	2.010	2.224	2.079 vw	
Liquid N_2	2.147	2.009	2.232	2.084 vw	2.066 vw
X = S	2.167	2.010		2.090 vw	
X = Se	2.163	2.012		2.095 vw	

[a] These values were taken from Q-band spectra as they are best resolved. [b] Crossover point is taken as $g_\perp$; high-field "bump" as $g_\parallel$. [c] Other spectral features than the $g_\perp$ absorption or the $g_\parallel$ bump are listed here by the location of the band center.

(27) P. C. Jain and E. C. Lingefelter, *J. Amer. Chem. Soc.*, 89, 724 (1967).

(28) B. J. Hathaway, D. E. Billing, R. J. Dudley, R. J. Fereday, and A. A. G. Tomlinson, *J. Chem. Soc. A*, 806 (1970).

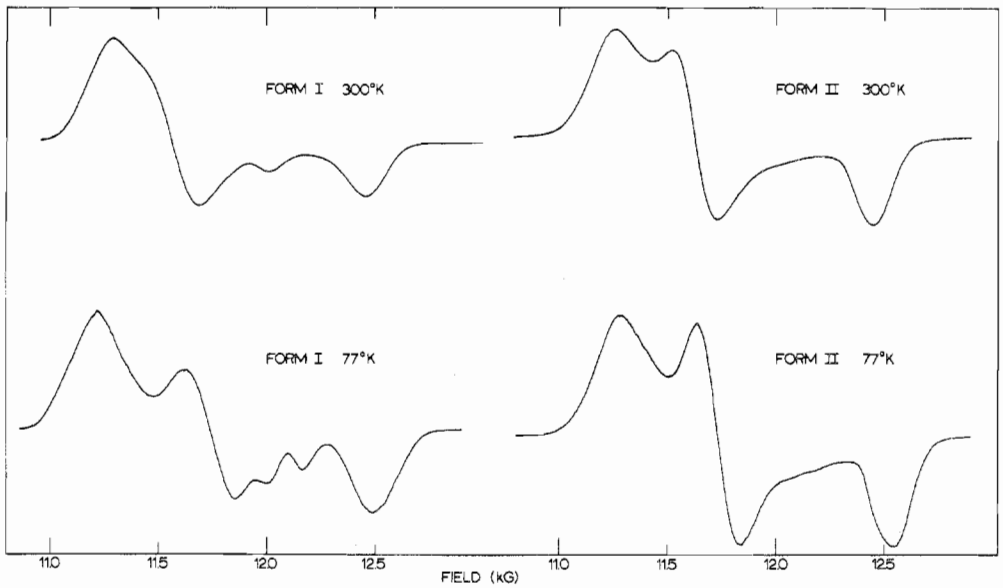

Figure 8. Q-Band (35.0 GHz) esr spectra of $[Cu_2(tren)_2(OCN)_2](BPh_4)_2$ forms I and II at room temperature and cooled with liquid nitrogen. The $\Delta M_S = \pm 1$ region is shown.

crystalline forms of $[Cu_2(tren)_2(NCO)_2](BPh_4)_2$ first became evident from a comparison of X-ray powder patterns for two samples of the compound that were obtained by different means. It is relevant to recall that the nickel cyanate compound also has two crystalline forms. The form I and form II copper cyanates have indistinguishable ir and electronic absorption characteristics and as such it can be concluded that, as result of the different packing in the two forms, there is probably a fairly subtle difference in the molecular structure of the copper cations in the two cases. Q-Band powder spectra of both form I and form II of $[Cu_2(tren)_2(NCO)_2](BPh_4)_2$ at room temperature and liquid nitrogen temperature are shown in Figure 8. Whereas X-band spectra for these two compounds show little structure, the Q-band spectra show considerable detail in the $\Delta M_S = 1$ region. For example, form I compound has an X-band spectrum with what appears to be overlapping parallel and perpendicular signals wherein the sign of the g anisotropy changes in decreasing the temperature from 300 to 77°K. Figure 8 shows, however, that the temperature dependence in the spectrum of form I is in fact much more complicated. We shall not attempt a detailed assignment of the g values at this time but shall note only that the g value associated with the highest field signal, presumably $g_\parallel$, is quite close (see Table VI) to 2.00 as expected for an undistorted trigonal-bipyramidal copper environment.[29] In each of the form I and II spectra in Figure 8 there are more than three features present (some are very weak and not readily discernible in the reproductions).

From the work of Smith and Pilbrow[30,31] it is known that complicated esr spectra may arise for a two-metal system when the **g** "tensor" is misaligned with the dipolar coupling (zero-field splitting) tensor. In other words, when the coordinate systems in which the **g** and **D** tensors are diagonalized are noncoincident, then extrema in the derivative esr spectrum may appear along directions which do not correspond to axes of either system. Such off-axis extrema may in fact be exemplified by the ~12.0-kG to 12.4-kG peaks observed in the form I copper cyanate spectra. Indeed the angle between the Cu-Cu vector and the trigonal axis of the copper trigonal bipyramid, taken as a measurement of the degree of **g**-**D** misalignment, is 36° (see Figure 7). It is expected that these off-axis extrema effects will be proportional in intensity to the size of the **D** tensor elements (which depend upon $1/d_{M-M}^3$), and as such one might conclude that for form II (Figure 8) either the copper atoms are farther apart or the degree of **g**-**D** misalignment is less. This argument must be weighted however by its apparent failure to explain the difference between the Q-band spectra of $[Cu_2(tren)_2(OCN)_2](BPh_4)_2$ and $[Cu_2(tren)_2(CN)_2](BPh_4)_2$,[26] where for the latter case $d_{Cu-Cu} = 6.090$ Å while the "**g**-**D**" angle (as defined above) is 44°, and yet no extra features are observed in the cyanide spectrum. These phenomena for undiluted powder samples are currently being investigated theoretically in these laboratories.

Q-Band powder spectra (77°K nominally) for $[Cu_2(tren)_2(SCN)_2](BPh_4)_2$ and $[Cu_2(tren)_2(SeCN)_2](BPh_4)_2$ are reproduced in Figure 9. There is very little temperature dependence observed for these samples, and low-temperature spectra are shown for their better resolution. The spectra for both materials show off-axis extrema and as such the close proximity of the metal atoms in each case is apparent. The weakness of these extra features for the selenocyanate compound correlates with the weakness of the $\Delta M_S = 2$ transition (see later discussion) and points out the larger metal-metal distance which is expected for this system.

From our above discussion we shall consider in the following sections that all three $[Cu_2(tren)_2(XCN)_2](BPh_4)_2$ compounds are dimeric by virtue of the XCN^- group being directly bonded to one copper and weakly bonding to a ligand in the coordination sphere of a second copper system. A characterization of the electronic exchange properties of such a dimer is tantamount to an investigation of the rate of an outer-sphere electron-transfer process between Cu(II) centers as it occurs in the solid state. In a very recent paper by Przystas and Sutin[32] the effect of added anions (*e.g.*, SCN^-) on the rates of outer-sphere redox reactions is reported. In

(29) B. J. Hathaway and D. E. Billing, *Coord. Chem. Rev.*, 5, 143 (1970).
(30) P. D. W. Boyd, A. D. Toy, T. D. Smith, and J. R. Pilbrow, *J. Chem. Soc., Dalton Trans.*, 1549 (1973).
(31) A. D. Toy, M. D. Hobday, P. D. W. Boyd, T. D. Smith, and J. R. Pilbrow, *J. Chem. Soc., Dalton Trans.*, 1259 (1973).
(32) T. J. Przystas and N. Sutin, *J. Amer. Chem. Soc.*, 95, 5545 (1973).

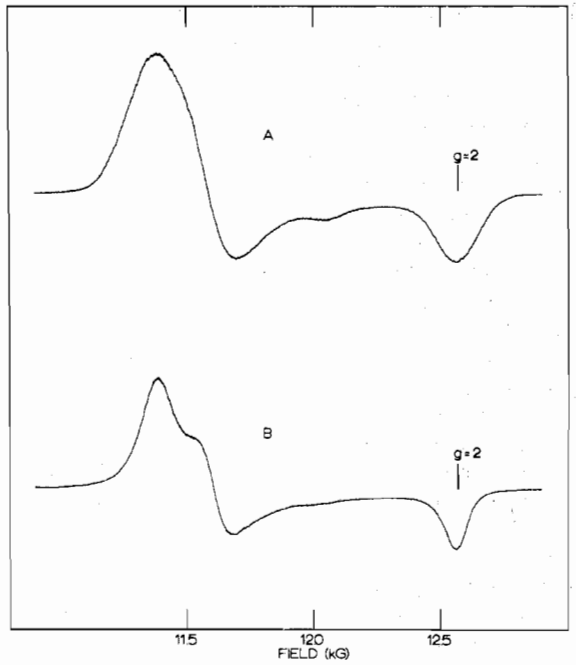

Figure 9. Q-Band (35.0 GHz) esr spectra of $[Cu_2(tren)_2(SCN)_2](BPh_4)_2$ (A) and $[Cu_2(tren)_2(SeCN)_2](BPh_4)_2$ (B) samples cooled with liquid nitrogen.

view of the rate effects observed by these workers it will be of interest to determine the exchange parameter J and thus qualitatively the electron-transfer rate for our systems as a function of the XCN^- group. We will first report attempts to characterize the exchange interaction using magnetic susceptibility studies, and then a detailed discussion of X-band esr studies on these systems will be presented in order to show both the quantum mechanical expectations and observed phenomena which have allowed us to determine the J values for the copper cyanate (forms I and II) and thiocyanate outer-sphere dimers.

The magnetic susceptibility results for the copper systems (see Table VII) are what might be expected from our previous study[4] of $[Cu_2(tren)_2(C_2O_4)](BPh_4)_2$ and $[Cu_2(tren)_2(N_3)_2](BPh_4)_2$. From 283 down to 4.2°K the effective magnetic moments of all of the copper compounds stay relatively constant, with only a small gradual decrease being observed for the lower temperature range ($\mu_{eff} \simeq 1.85$ BM at 4.2°). The exchange interactions are apparently very weak in these XCN^--Cu complexes.

Before presenting the esr results we will briefly sketch the theoretical background requisite to make these results more meaningful. For a system in which pairs of copper(II) ions are interacting, the esr spectrum can be described by the spin Hamiltonian

$$\hat{H} = g\beta H(S_{1z} + S_{2z}) + A(\hat{S}_1 \cdot \hat{I}_1 + \hat{S}_2 \cdot \hat{I}_2) + \hat{H}_D - 2J\hat{S}_1 \cdot \hat{S}_2 \quad (1)$$

Here g is the g factor, β is the Bohr magneton, H is the applied magnetic field, $\hat{S}_1$ and $\hat{S}_2$ are the spin operators of the two copper electrons, $\hat{I}_1$ and $\hat{I}_2$ are the nuclear spins, A is the hyperfine coupling constant, H_D is the Hamiltonian for dipolar coupling, and J is the exchange parameter. Anisotropy of g has been ignored for this illustration, and the exchange term is written so as to be consistent with that used in the nickel magnetic susceptibility work. Eigenfunctions of the first and fourth terms in H may be written

$$|{}^1/_2\,{}^1/_2\rangle \equiv |11\rangle \quad (2)$$

$$(1/\sqrt{2})(|{}^1/_2 - {}^1/_2\rangle + |-{}^1/_2\,{}^1/_2\rangle) \equiv |10\rangle \quad (3)$$

$$|-{}^1/_2 - {}^1/_2\rangle \equiv |1-1\rangle \quad (4)$$

$$(1/\sqrt{2})(|{}^1/_2 - {}^1/_2\rangle - |-{}^1/_2\,{}^1/_2\rangle) \equiv |00\rangle \quad (5)$$

where the kets on the left are in the uncoupled $|M_{S_1} M_{S_2}\rangle$ notation and those on the right are the coupled basis set $|SM_S\rangle$, $S = S_1 + S_2$. Using only the Zeeman and exchange terms of the Hamiltonian, these four functions would give rise to a triplet ($S = 1$) and a singlet ($S = 0$) state, separated by $2J$ at zero field, with a magnetic field dependence as indicated in Figure 10. With the microwave excitation field perpendicular to H, the static field, the allowed transitions with this simple two-term Hamiltonian are only $|1-1\rangle \rightarrow |10\rangle$ and $|10\rangle \rightarrow |11\rangle$ (both $\Delta M_S = 1$), which are of equal energy with the neglect of zero-field interaction. The effects of including $\hat{H}_D$ have been treated in detail elsewhere.[33] With $\hat{H}_D$, $|10\rangle$ is no longer degenerate with $|11\rangle$ and $|1-1\rangle$ in zero field and the $\Delta M_S = 2$ transition becomes weakly allowed, giving a resonance at half the magnetic field required to see the $\Delta M_S = 1$ absorption.

Addition of nuclear hyperfine $\hat{H}' = A(\hat{S}_1 \cdot \hat{I}_1 + \hat{S}_2 \cdot \hat{I}_2)$, or for the isotropic case $\hat{H}' = A(S_{1z}I_{1z} + S_{2z}I_{2z})$, results in the matrix elements

$$\langle 11M_{I_1}M_{I_2}|\hat{H}'|11M_{I_1}M_{I_2}\rangle = (A/2)(M_{I_1} + M_{I_2}) \quad (6)$$

$$\langle 1-1M_{I_1}M_{I_2}|\hat{H}'|1-1M_{I_1}M_{I_2}\rangle = (-A/2)(M_{I_1} + M_{I_2}) \quad (7)$$

$$\langle 10M_{I_1}M_{I_2}|\hat{H}'|00M_{I_1}M_{I_2}\rangle = \langle 00M_{I_1}M_{I_2}|\hat{H}'|10M_{I_1}M_{I_2}\rangle = (A/2)(M_{I_1} - M_{I_2}) \quad (8)$$

Solving the 2×2 matrix in $|00\rangle$ and $|10\rangle$, including the Zeeman and exchange interactions but ignoring zero-field splitting (it is energetically a small effect in our systems), leads to the eigenfunctions and eigenvalues

$$|10M_{I_1}M_{I_2}\rangle' = |10M_{I_1}M_{I_2}\rangle - (A/4J)(M_{I_1} - M_{I_2}) \times |00M_{I_1}M_{I_2}\rangle \quad (9)$$

$$E_{10'} = J/2 - (A/4J)(M_{I_1} - M_{I_2}) \quad (10)$$

$$|00M_{I_1}M_{I_2}\rangle' = |00M_{I_1}M_{I_2}\rangle + (A/4J)(M_{I_1} - M_{I_2}) \times |10M_{I_1}M_{I_2}\rangle \quad (11)$$

$$E_{00'} = -{}^3/_2 J + (A/4J)(M_{I_1} - M_{I_2}) \quad (12)$$

While the inclusion of the nuclear hyperfine has slightly affected the energies of $|10\rangle$ and $|00\rangle$, it has made the transition moment integrals $\langle 00|I_x + I_y|11\rangle$ and $\langle 1-1|I_x + I_y|00\rangle$ nonzero. The energies of these singlet to triplet transitions are

$$E_1 = g\beta H + 2J - (A^2/16J)(M_{I_1} - M_{I_2})^2 \quad (13)$$

$$E_2 = g\beta H - 2J - (A^2/16J)(M_{I_1} - M_{I_2})^2 \quad (14)$$

and their intensities are proportional to $|\langle 00|I_x + I_y|11\rangle|^2 = (A^2/4J^2)(M_{I_1} M_{I_2})^2$. Thus electron-nuclear coupling can lead to the observation of normally forbidden transitions whose field positions will be approximately $\pm 2J/g\beta$ from the $\Delta M_S = 1$ transition (approximate because of the small A^2 term) and whose intensities depend on $(A^2/J^2)(M_{I_1} - M_{I_2})^2$. The $(M_{I_1} - M_{I_2})$ term is interesting, for it says that when the two copper atoms are not magnetically equivalent, the $|M_{S_1}$·

(33) J. F. Boas, R. H. Dunhill, J. R. Pilbrow, R. C. Srivastava, and T. D. Smith, *J. Chem. Soc. A*, 94 (1969).

Table VII. Experimental Magnetic Susceptibility Data for $[Cu_2(tren)_2(XCN)_2](BPh_4)_2$ (X = O, S, Se)[a]

	X = O		X = S		X = Se	
T, °K	$10^3\chi_M$	μ_{eff}/Cu	$10^3\chi_M$	μ_{eff}/Cu	$10^3\chi_M$	μ_{eff}/Cu
283.0	3.758	2.062	4.046	2.140	3.677	2.040
247.7	4.303	2.065				
218.3	4.890	2.066	4.973	2.083		
188.4	5.572	2.049			5.262	1.991
156.7	6.500	2.018	6.639	2.040		
117.2	8.301	1.973	8.574	2.004	8.089	1.947
73.6	13.01	1.957	13.14	1.966	12.71	1.935
59.5	15.96	1.949	16.54	1.984	16.18	1.962
47.8	19.22	1.917	20.07	1.959	19.69	1.940
31.5	28.54	1.896	31.70	1.998	31.20	1.983
26.0			36.94	1.960	36.36	1.945
20.5	44.98	1.920	45.10	1.923	44.40	1.908
15.7	57.88	1.907	57.99	1.908	57.14	1.894
11.7	74.20	1.864	74.29	1.864	73.41	1.853
9.3	93.95	1.869	93.85	1.868	92.53	1.855
7.3	118.7	1.862	118.0	1.856	117.3	1.850
5.6	154.0	1.858	154.2	1.858	150.4	1.835
4.7	178.6	1.832	178.9	1.834	175.7	1.817
4.2	203.8	1.851	206.6	1.862	201.8	1.841

[a] χ_M in cgsu/mol; μ_{eff} in BM. Form I (powder) cyanate data reported. Diamagnetic corrections: cyanate, -687.7×10^{-6} cgsu; thiocyanate, -708.1×10^{-6} cgsu; selenocyanate, -721.7×10^{-6} cgsu.

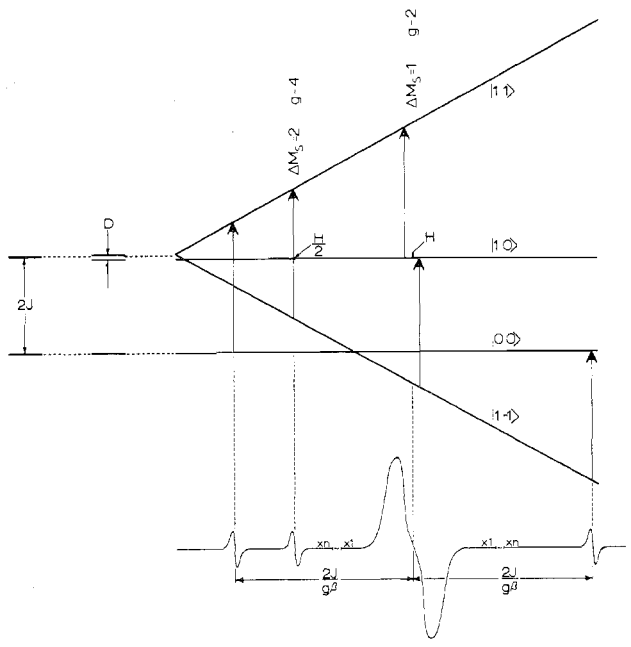

Figure 10. Illustration of idealized energy level scheme and esr spectrum for two $S = {}^1/_2$ systems interacting to show both zero-field splitting D and exchange coupling J. Allowed transitions ($\Delta M_S = 1$) are shown as large derivative features in the spectrum, whereas formally forbidden ($\Delta M_S = 2$ and singlet to triplet state) transitions are shown at an increased spectrometer gain (*i.e.*, n times greater).

$M_{S_2}\rangle$ descriptions $|{}^1/_2 -{}^1/_2\rangle$ and $|-{}^1/_2 {}^1/_2\rangle$ are distinguishable and as a result the spin functions in eq 3 and 5 do not have the symmetry of the molecule unless they are slightly mixed.

The idealized esr spectrum expected from a $S' = 1$ dimer system is illustrated in Figure 10. In practice, $\Delta M_S = 2$ transitions are expected mainly for dimers with Cu-Cu distances between ~3 and ~5 Å.[33] This is because the zero-field split components of the $\Delta M_S = 1$ transition will overlap the $\Delta M_S = 2$ band when the Cu-Cu distance is small, making it unobservable. When the Cu-Cu distance is large and the zero-field parameter D is thus small (dipolar term depends on d^{-3}), the intensity of the $\Delta M_S = 2$ absorption will be low. The Cu-Cu distance in $[Cu_2(tren)_2(OCN)_2](BPh_4)_2$ is 6.58 Å and the $\Delta M_S = 2$ transition is roughly 0.001 as large as the $\Delta M_S = 1$ transition. The observation of singlet-triplet transitions turns out to be a rather rare event. They have been reported,[18] as mentioned in the Introduction, in only one copper dimer, but this reporting was not, in our opinion, properly substantiated. It is obvious that J values of only a limited size (less than the microwave quantum) can be measured with the esr technique. The esr spectra for the $[Cu_2(tren)_2(XCN)_2](BPh_4)_2$ compounds show no readily assignable zero-field splitting in the $\Delta M_S = 1$ absorption which follows from the magnitudes of the Cu-Cu distances that are involved. In reference to $\Delta M_S = 2$ and singlet-to-triplet transitions, the esr results for copper cyanate, thiocyanate, and selenocyanate systems are presented individually below.

Figure 11 shows a wide-range (0–10,000 G) X-band esr spectrum of pure form I of $[Cu_2(tren)_2(NCO)_2](BPh_4)_2$ at two temperatures. The notable features of these spectra are (1) the presence of a $\Delta M_S = 2$ transition suggesting the proximity of two copper atoms, (2) the asymmetry of the $\Delta M_S = 1$ feature (note that the g anisotropy actually *appears* to change sign as a function of temperature; however the previous section on the Q-band spectra should be recalled), and (3) singlet-triplet transitions. In the 345°K spectrum the two S → T transitions are readily detectable and their positions give $|J| = 0.09$ cm^{-1}. Lowering the temperature leads to a pronounced movement of the two S → T transitions to lower and higher field positions and at 95°K one finds $|J| = 0.16$ cm^{-1}, which is approaching the largest J that can be detected with X-band esr.

The temperature dependence of the X-band esr spectrum of pure form II of $[Cu_2(tren)_2(NCO)_2](BPh_4)_2$ is shown in Figure 12. Again a $\Delta M_S = 2$ band is noted. There are two differences between the form I and form II spectra. The $\Delta M_S = 1$ absorption for form II does not seem to change so radically in shape as it does for form I. In addition, the singlet-triplet transitions for form II are closer to the $\Delta M_S = 1$ peak and do not seem to move as much with decreasing temperature. The temperature dependences of the exchange parameters for the two forms of $[Cu_2(tren)_2(NCO)_2](BPh_4)_2$ are illustrated in Figure 13. As it is unusual to have a determination of the temperature dependence of J, we will discuss the probable mechanisms for this dependence. It has been suggested that J values may change with dimensional changes in a system, where the dimensional changes can result either from lattice shrinkage effects[17,34] or from magnetostriction[35] (the change of bridge dimensions as a system goes into its magnetically ordered state), or they may be due to a more subtle solid-state effect.[17,34] Because the magnetostriction effect would only be seen for strongly coupled cases ($J \geq 10$ cm^{-1} in order to have an appreciable order at 4.2°K), only lattice shrinkage would be operative in the two copper cyanates. It is clear from Figure 12 that not only is the J temperature dependence greater for form I but also there is reversal in curvature of the J *vs.* T curve. The bridge bonding in form I is sufficiently different from that in form II to yield a J that is much more dimensionally sensitive. To our knowledge there are no discussions in the literature as to the functionality of the dependence of J on changes in the dimensions of the bridge.

It seems reasonable that, given the hydrogen-bonded character established for form I, there could be a fairly tempera-

(34) T. A. Kennedy, S. H. Choh, and G. Seidel, *Phys. Rev. B*, 2, 3645 (1970).
(35) M. E. Lines, *Solid State Commun.*, 11, 1615 (1972).

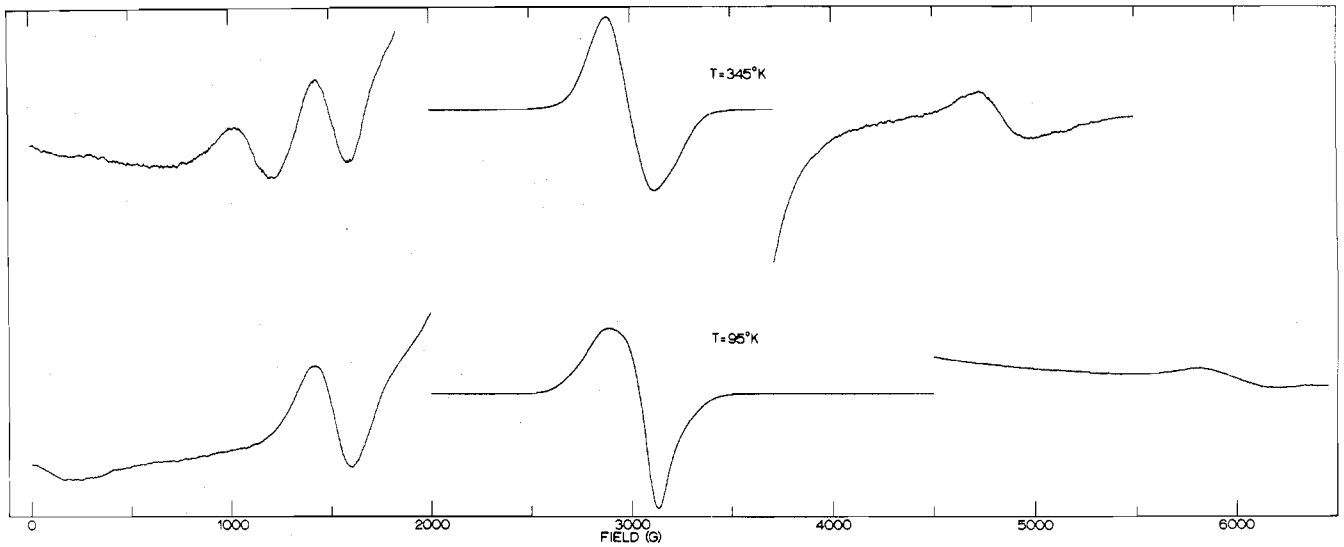

Figure 11. Temperature dependence of all visible features in the X-band (9 GHz) esr spectrum of $[Cu_2(tren)_2(OCN)_2](BPh_4)_2$ form I.

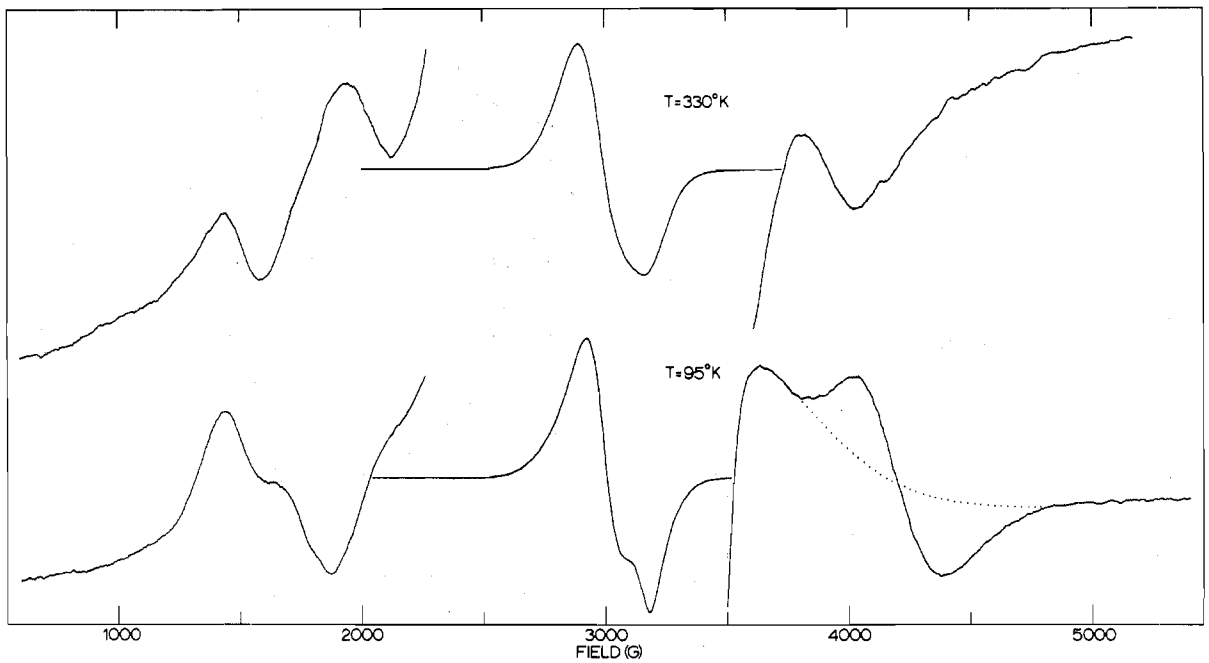

Figure 12. Temperature dependence of all visible features in the X-band (9 GHz) esr spectrum of $[Cu_2(tren)_2(OCN)_2](BPh_4)_2$ form II.

ture-dependent J value. Thus the $[Cu_2(tren)_2(NCO)_2]^{2+}$ dimensional changes enforced by lattice shrinkage might be absorbed in large part by the hydrogen bond linkage, and because the exchange is propagated *via* this bond, the J value changes with temperature. Inspection of Figure 7 shows that the form I dimer has a tren ligand configuration wherein the ethylene rings are in conformations that preserve the threefold symmetry of the Cu(tren) moiety. The tren nitrogen which is involved in the hydrogen bonding actually has two types of hydrogens (as do the other two radial nitrogens), one oriented perpendicular to the CuN_3 radial plane and the other roughly in the plane. It is the former hydrogen which is involved in the hydrogen bonding in the room-temperature form I compound. Speculation as to the molecular structure of form II dimer could include a structure where one of the tren "arms" is in a different conformation, a structure where the hydrogen bonding is effected through the in-plane hydrogen atom, or a structure where basically the *same* dimer structure as form I is realized but because of a different packing with the tetraphenylborate ions the hydrogen-bond distance is longer leading to a smaller J value. It remains for crystallographic studies to define the mode of bridging in the form II copper cyanate.

Table VIII. Summary of J Values (cm^{-1}) for Copper Systems

$[Cu_2(tren)_2(OCN)_2](BPh_4)_2$	
Form I	0.09–0.16[a]
Form II	0.05–0.06
$[Cu_2(tren)_2(SCN)_2](BPh_4)_2$	0.05–0.07
$[Cu_2(tren)_2(SeCN)_2](BPh_4)_2$	Not detectable

[a] Temperature dependent as described in text.

The esr spectra of $[Cu_2(tren)_2(SCN)_2](BPh_4)_2$ are quite similar to that for form II of the copper cyanate species, in that more than three features are visible in the (powder) Q-band $\Delta M_S = 1$ region and one observes a $\Delta M_S = 2$ and singlet-to-triplet transitions (the J value is given in Table VIII along with those for the cyanates). The J value for the thiocyanate complex is similar to that for form II of the cyanate and as such its molecular structure may also be analogous. The temperature dependence of the thiocyanate J value is

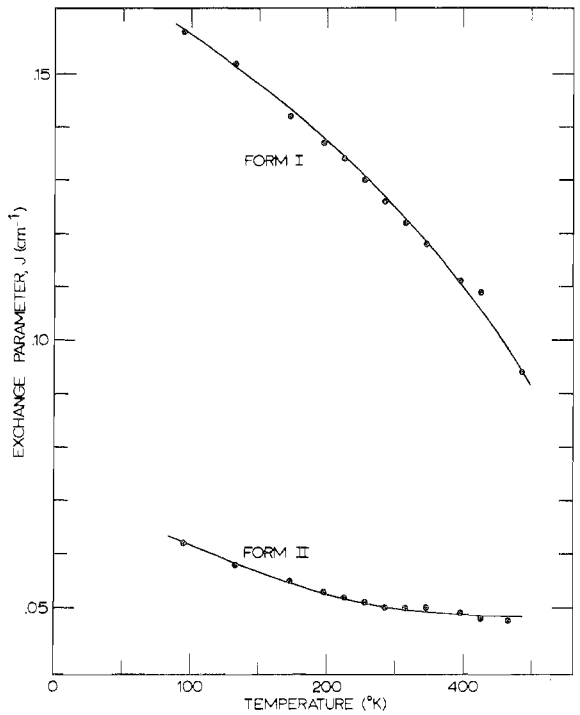

Figure 13. Temperature dependence of the J values of $[Cu_2(tren)_2(OCN)_2](BPh_4)_2$ forms I and II, as determined by study of singlet–triplet esr transitions.

slight, being comparable to that for form II cyanate.

For the selenocyanate complex we find a notably weaker $\Delta M_S = 2$ transition for the pure compound, and (see Table VIII) no singlet–triplet transitions are observed. The latter are presumed to be obscured by the $\Delta M_S = 1$ absorption. This is in keeping with our earlier discussion concerning the structure of the selenocyanate dimer.

Conclusion

Nickel(II) and copper(II) complexes of the composition $[M_2(tren)_2(XCN)_2](BPh_4)_2$ (X = O, S, Se) have been studied; the nickel complexes have been shown to be octahedral by virtue of di-XCN bridging, whereas the copper complexes are trigonal bipyramidal yet dimeric due to *outer-sphere* bridging. In the case of the nickel complexes the symmetry of the XCN bridging group determines the *sign* and *magnitude* of the exchange parameter J, which is for these complexes in the range -5 to $+3$ cm^{-1}. For the outer-sphere copper dimers the J values are much smaller and are quite sensitive to dimensional changes in the bridge, as indicated by the temperature dependence. While the nickel systems clearly illustrate factors of key importance when studying electron exchange which depends upon the interactions of two *directly* bridged metals in the solid state, the copper systems point out that, even for metal ions interacting through outer-sphere coordination, exchange can be appreciable. Furthermore, the dimensional sensitivity of this outer-sphere exchange provides some insight into the magnitude of transition-state structural changes which might have appreciable effect on the rates observed for solution outer-sphere redox reactions.

Experimental Section

Preparation of Compounds. All six of the $[M_2(tren)_2(XCN)_2](BPh_4)_2$ (M = Cu, Ni; X = O, S, Se) materials reported herein may be prepared by the procedure outlined as follows. Dissolve 0.01 mol of $MSO_4 \cdot nH_2O$ in ~100 ml of water and then add a solution (~50 ml) of the appropriate *sodium* XCN salt. The solution is stirred, and upon addition of 1.5 ml of tren (Ames laboratories) followed by ~0.5 g of $NaBPh_4$ dissolved in 30 ml of water, a precipitate is instantly formed which is filtered, washed several times with water, then washed with ether, and dried *in vacuo* over P_2O_5.

Crystals of the nickel cyanate and copper compounds were obtained by slow evaporation of an acetonitrile solution. As indicated in the body of the paper the crystals obtained for the nickel cyanate complex have a different crystallographic structure than that for the powdered material. This phenomenon is repeated for the copper cyanate; however for this system the crystalline material is composed of crystals of two different types: one is needlelike, while the other is larger and more equilateral in shape but not of clearly defined form. Separation of the two forms of crystals under a microscope produced samples that could be identified as form I for the needles and form II for the larger crystals. This identification is most readily accomplished using the esr properties of the systems.

The sample of $Ni(tren)(SCN)_2$ was prepared from a water solution of equimolar amounts of $NiSO_4 \cdot 6H_2O$ and tren to which was added excess NaSCN. *Anal.* Calcd for $C_8H_{18}N_6S_2Ni$: C, 29.92; H, 5.65; N, 26.17; Ni, 18.28. Found: C, 30.18; H, 5.70; N, 26.46; Ni, 18.41.

Microanalyses were obtained from the University of Illinois School of Chemical Sciences microanalytical laboratory.

Physical Measurements. Infrared spectra were recorded on a Perkin-Elmer Model 457 spectrophotometer using 13-mm KBr pellets containing ~1% sample. Electronic spectral data were obtained for similarly pelleted samples on a Cary 14 spectrometer (only 90 mg of KBr was used). In view of the large dispersion and high-energy absorption effects obtained for these samples, in order to observe adequately defined sample absorptions in the visible region it was necessary to place a ~1 mg of $NaBPh_4$/90 mg of KBr pellet in the reference beam of the spectrophotometer. X-Ray powder patterns for all samples were recorded on a Philips-Norelco powder diffractometer unit using a photon counter and Cu Kα radiation. The samples were prepared as evaporated benzene slurries on glass microscope slides. X-Band esr spectra were taken using a Varian E-9 spectrometer with a 10-kG magnet. Variable-temperature studies were accomplished using a liquid nitrogen cooled dry nitrogen gas stream to cool the sample and a temperature control unit, the accuracy of which is probably not better than ±10°K. Most of the data points for the temperature dependence of the cyanate J values (shown in Figure 13) were taken from a set of spectra of a *mixture* of forms I and II in the same sample, and as such the *relative* curvatures and temperature variations are well represented. Q-Band data were obtained using a Varian 35-GHz microwave bridge with a 12-in. Varian magnet capable of fields up to 24 kG. Low-temperature spectra were taken with a narrow-necked glass dewar surrounding the cavity and yet inside the cylindrical modulation coils. With the dewar pushed up until its top was ~2 in. above the top of the cavity it could be filled with liquid nitrogen until the cavity was completely immersed. The sample tube was inserted into the cavity such that its end was in a silicone grease filled hole in the cavity bottom. In this way maximum thermal conduction was ensured and the sample temperature was *nominally* 77°K.

Magnetic susceptibility data were collected using a Princeton Applied Research Model 150A vibrating-sample parallel-field magnetometer fitted with a Janis liquid helium dewar and Westinghouse 50-kG superconducting solenoid.

Acknowledgment. We are very grateful for support from National Institutes of Health Grant HEW PHS HL13652. The Varian X- and Q-band esr facilities were purchased, in part, by a departmental NSF grant.

Registry No. $[Ni_2(tren)_2(OCN)_2](BPh_4)_2$, 49660-74-4; $[Ni_2(tren)_2(SCN)_2](BPh_4)_2$, 52571-25-2; $[Ni_2(tren)_2(SeCN)_2](BPh_4)_2$, 52571-27-4; $[Cu_2(tren)_2(OCN)_2](BPh_4)_2$, 52699-44-2; $[Cu_2(tren)_2(SCN)_2](BPh_4)_2$, 52665-52-8; $[Cu_2(tren)_2(SeCN)_2](BPh_4)_2$, 52665-54-0.

Supplementary Material Available. Tables I, II, and IV, containing analytical ir, and magnetic susceptibility data, will appear following these pages in the microfilm edition of this volume of the journal. Photocopies of the supplementary material from this paper only or microfiche (105 × 148 mm, 24× reduction, negatives) containing all of the supplementary material for the papers in this issue may be obtained from the Journals Department, American Chemical Society, 1155 16th St., N.W., Washington, D. C. 20036. Remit check or money order for $3.00 for photocopy or $2.00 for microfiche, referring to code number INORG-74-2929.